Electroacupuncture alleviates MIRI by regulating hypothalamic paraventricular nucleus neurons projecting to the rostral ventrolateral medulla

Qi Shu[a,1], Jie Zhou[b,1], Bin Zhang[b], Fan Zhang[a], Xiang Zhou[b], Yan Wu[b], Huimin Chang[b], Ling Hu[b,c], Ronglin Cai[c,d,*], Qing Yu[c,d*]

[a] *College of Traditional Chinese Medicine, Anhui University of Chinese Medicine, 103 Meishan Road, Hefei 230031, China*

[b] *Medical College of Acu-Moxi, Anhui University of Chinese Medicine, 103 Meishan Road, Hefei 230031, China*

[c] *Institute of Acupuncture and Moxibustion Meridian*, *Anhui University of Chinese Medicine, 103 Meishan Road, Hefei 230031, China*

[d] *Anhui Province Key Laboratory of Meridian Viscera Correlationship, Anhui University of Chinese Medicine, 103 Meishan Road, Hefei 230031, China*

[*]Corresponding authors.

E-mail adress: ronglincai@163.com (R-L Cai), yuqingtcm@126.com (Q Y)

[1] These authors have contributed equally to this work and share the first authorsip.

Abstract

Accumulating evidence suggests that electroacupuncture (EA) has obevious therapeutic effects and unique advantages in alleviating myocardial ischemia-reperfusion injury (MIRI), while the underlying neuromolecular mechanisms of EA intervention for MIRI have not been fully elucidated. The aim of the study is to investigate the role of the neural pathway of hypothalamic paraventricular nucleus (PVN) neurons projecting to the rostral ventrolateral medulla (RVLM) in the alleviation of MIRI rats by EA preconditioning. MIRI models were established by ligating the left anterior descending coronary artery for 30 min followed by reperfusion for 2 h. Electrocardiogram recording, chemogenetics, enzyne-linked immunosorbent assay, multichannel physiology recording, hematoxylin-eosin and immunofluorescence staining methods were conducted to demonstrate that firing frequencies of neurons in the PVN and expression of c-Fos decreased by EA pretreatment. Meanwhile, EA preconditioning significantly reduced the levels of creatine kinase isoenzymes (CK-MB), cardiac troponin I (cTnI) and lactic dehydrogenase (LDH). Virus tracing showed a projection connection between PVN and RVLM. Inhibition of the PVN-RVLM neural pathway could replicate the protective effect of EA pretreatment on MIRI rats. However, activation of the pathway weakened the effect of EA preconditioning. EA pretreatment alleviated MIRI by regulating PVN neurons projecting to RVLM. This work provides novel evidence of EA pretreatment for improving MIRI.

Key words: Electroacupuncture (EA), Myocardial ischemia-reperfusion injury (MIRI), hypothalamic paraventricular nucleus, rostral ventrolateral medulla, neural pathway

1. Introduction

Ischemic heart disease is a major component of cardiovascular disease with high morbidity and mortality, causing a huge burden of disease to public health worldwide. It's reported that the number of cardiovascular diseases worldwide has almost doubled from 271 million in 1990 to 523 million in 2019[1]. In China, there were 40.7 cardiac deaths per 100,000 person-years from 1980 to 2016[2]. Reperfusion therapy, as a routine clinical treatment for myocardial ischemia, can effectively rescue the hypoxic state of myocardial ischemia, but the accompanying inflammatory reactions and calcium overload will further exacerbate myocardial injury[3]. which called myocardial ischemia-reperfusion injury (myocardial ischemia-reperfusion injury, MIRI). MIRI play essential functions in ischemic heart disease, which refers to a complex pathophysiological process that includes depletion of adenosine triphosphate[4], excessive generation of reactive oxygen species[5], inflammatory reactions[6], and mitochondrial dysfunction owing to clacium overload[7], which triggers acute myocardial infarction via metabolic dysfunction and structural damage[8]. Given the various mechanism and accompanying symptoms, effective anti-MIRI methods are still a huge challenge.

As a traditional Chinese alternative health care approach, acupuncture is gaining increasing attention and reputation around the world. A large amount of evidence shows that acupuncture has a significant effect on the treatment of cardiovascular diseases[9-11]. Specially, acupuncture pre-treatment serves as a "benign stress" method to activate the body's immune system and improve self-defense or tolerance to resist the invasion of subsequent diseases, which provides a promising intervention for prevention and treatment of MIRI. Furthermore, various studies have shown that the phenomenon of acupoint acupuncture sensation is essentially a neural sensation[12], which suggests that the transmission of acupuncture information depends on the nervous system. In fact, acupuncture at acupoints and non acupoints can cause two activation modes in different regions of the brain by functional magnetic resonance imaging (fMRI) technology[13,14]. Previous studies have revealed that the hypothalamic limbic system has a positive response to acupuncture pretreatment for improving MIRI, which aroused our interest[15,16].

The paraventricular nucleus (PVN), an important integrative site for the control of cardiovascular activity, contains neurons that project to the intermediolateral cell column of the thoracolumbar spinal cord and the rostral ventrolateral medulla (RVLM)[17]. Studies have shown that PVN controls sympathetic nerve activity and blood pressure[18-20], which may be a underlying target for acupuncture treatment of cardiovascular diseases. Coronary ligation is one of the sources of afferent input to the PVN[21,22]. Our previous study have also discovered that PVN is one of the central regulatory targets of the heart by retrograde virus tracing (unpublished). Therefore, we try to explore the mechanism of PVN in electroacupuncture pretreatment alleviating MIRI neurogically.

2. Materials and methods

2.1 Animals and ethics

Male Sprague-Dawley rats weighing 220±20g were purchased from Jinan Pengyue Experimental Animal Breeding Co., Ltd.(Shandong province, China, Certificate No.SCXK (Lu) 2019-003). The rats were housed in the animal center of Anhui University of Traditional Chinese Medicine and fed adaptively in cages under the

same conditions for one week(24±2℃;55 ± 5 % humidity; 12 h light/dark cycle). All experiments were approved by the Animal Experiment Ethics Committee of the Anhui University of Traditional Chinese Medicine(No.AHUCM-rats-2020028). The study was carried out in accordance with the ARRIVE guidelines.

2.2 Animal grouping and experimental design

First, the rats were randomly (Analysis Toolpak) divided into three groups which are outlined below: 1) in the sham operation group (Sham, n=24), the rats were narcotized by isoflurane for 20 min a day for 7 consecutive days. On the eighth day, they underwent a sham surgery, consisting of left thoracotomy but without the ligation of the left anterior descending (LAD) coronary artery. 2) In the MIRI model group (Model, n=24), the rats were also narcotized by isoflurane for 20 min a day for 7 continuous days without EA treatment. On the eighth day, MIRI model was induced by ligating the LAD for 30 min, followed by 2 h of reperfusion. 3) In the EA pretreatment group (EA, n=24), the rats were narcotized by isoflurane for 20 min a day for 7 consecutive days with EA (20Hz, 0.5mA) at bilateral “Shenmen” (HT7). MIRI operation was performed on the eighth day.

Second, 6 rats were injected rAAV-hSyn-mCherry-WPRE-hGH polyA in the PVN (n=3) and CTB-555 in the RVLM (n=3) to verify the connection between PVN and RVLM.

Third, 84 rats were all injected chemogenetics virus and randomly divided into seven groups as follows:1) In the virus control group (sham+mCherry+CNO, n=12), rats were under brain injection of rAAV-EF1α-DIO-mCherry-WPRE-hGH pA in PVN and retroAAV-hSyn-CRE-WPRE-hGH pA in RVLM bilaterally, after 21 days, they were narcotized by isoflurane for 20 min a day for 7 consecutive days without any invention, clozapine N-oxide (CNO) was injected intraperitoneally before sham operation on the eighth day. 2) In the virus model group (model+mCherry+CNO, n=12), the treatment was the same as that of the virus control group except for the MIRI operation on the eighth day. 3) In the inhibitory virus group (model+hM4Di+CNO, n=12), rats were injected rAAV-EF1α-DIO-hM4D(Gi)-mCherry-WPREs in PVN and retroAAV-hSyn-CRE-WPRE-hGH pA in RVLM bilaterally, underwent anesthesia without EA treatment for 7 consecutive days after 21 days from injection. CNO was injected intraperitoneally before MIRI operation on the eighth day. 4) In the inhibitory virus control group (model+hM4Di+Saline, n=12), the measures were the same as those of inhibitory virus group except the injection of saline on the eighth day. 5) In the virus EA group (EA+mCherry+CNO, n=12), 21 days after injection, rats were narcoized and injected CNO 30 min before starting each EA treatment. MIRI operation was performed on the eighth day. 6) In the excitatory virus group (EA+hM3Dq+CNO, n=12), rats were injected rAAV-Ef1α-DIO-hM3D(Gq)-mCherry-WPREs in PVN and retroAAV-hSyn-CRE-WPRE-hGH pA in RVLM bilaterally. Injected CNO 30 min before each EA treatment after 21 days and performed MIRI operation on the eighth day. 7) In the excitatory virus control group (EA+hM3Dq+Saline, n=12), the interventions were the same as the excitatory virus group except for the injection of saline.

2.3 EA intervention

Only the rats in the EA group received EA intervention before MIRI modeling. EA was applied at *Shenmen* acupoint (HT7) for 30 min everyday for continuous 7 days . HT7 was located on the ulnar side of the rat wrist. After routinely sterilizing wrist skin, we inserted an acupuncture

needle to HT7, another needle was inserted 2 mm adjacent to HT7. The needling depth is 3mm. The EA apparatus (continuous wave; current, 1mA; frequency, 2Hz; HANS-200A/100B; HANS, Beijing, China) was attached to the acupuncture needle.

2.4 Establishment of MIRI model

Rats were anesthetized by 3% isoflurane with 99.5% O2 and maintained under anesthesia by 1.5-2% isoflurane. Using a Powerlab multichannel physiological recorder, the standard Ⅱ lead electrocardiogram of rats was recorded. The neck and chest were prepared for the surgical field, tracheal intubation was performed, and an animal ventilator was connected (respiratory frequency 90 times/min, inspiratory ratio 1:2, tidal volume 1.1).Cutting the skin from the third to fourth intercostal space, bluntly separated the muscle tissue, opened the thoracic cavity, cut the pericardium, and the LAD coronary artery was occluded with a 6.0 silk suture for 30 min followed by 120 min of reperfusion. Successful occlusion was confirmed by the development of a cyanotic anterior ventricular wall, elevated ST segments, and peaked T-waves on the ECG.

2.5 Arrhythmia score

We used the Curtis-Walker arrhythmia scoring method to evaluate the arrhythmia scores within 10 min after re-perfusion in each group. The scoring criteria are as follows: normal score is 0 point, atrial arrhythmias or occasional ventricular premature beats are 1 point (less than 3 occurrences per minute), frequent ventricular premature beats are 2 points (more than or equal to 3 occurrences per minute), 1-2 series of ventricular tachycardia are 3 points (less than 3 occurrences per minute), and more than 3 series of ventricular tachycardia (more than or equal to 3 occurrences per minute) or occasional ventricular fibrillation (less than 3 occurrences per minute) are 4 points, Frequent ventricular fibrillation (≥ 3 occurrences per minute) or death: 5 points.

2.6 Perfusion and tissue sectioning

After modeling, rats were anesthetized deeply and perfused transcardially with 0.9% cold saline (Xinhe Yuansheng Pharmaceutical Co., Ltd, Henan, China), followed by 4% paraformaldehyde (PFA) (Biosharp, Anhui, China) in PBS (BasalMedia, Shanghai, China). After the liver of the rat turned white and the limbs twitched, we took out the heart and then cut off the head to take out the brain. The brains were postfixed overnight in 4% PFA at 4C, and cryopreserved in 20% and 30% sucrose in PBS, and then embedded in Tissue-Tek OCT (Sakura, Japan) compound. Each brain (40 μm) was cut in the transverse plane using a freezing microtome (Leica, Germany).

2.7 Hematoxylin-eosin (HE) staining

The heart tissue was fixed in PFA for 24 h, all samples were embeded in paraffin before cutting into 5 μm sections, and then the sections were stained with hematoxylin and eosin for observation with an Olympus microscope (Olympus Corporation, Japan).

2.8 Enzyme-link immunosorbent assay

According to the manufacturer, CK-MB, LDH and cTnI concentration were determined by Sandwich-ELISA using the rat CK-MB, LDH and cardiac cTnI ELISA kits (Cat. No. JYM0716Ra, JYM0024Ra, JYM0309Ra, Wuhan jiyinmei, China).

2.9 Immunostaining

Free-floating sections were washed three times with PBS for 5 min each time, incubated for 1 h in blocking solution (3%BSA; Spark Jade, Shandong, China) at 37℃ and 0.3% Triton X-100 (Biosharp, Anhui, China) in PBS and incubated overnight at 4℃ with primary antibodies (anti-c-Fos, 1:500, Univ, Shanghai, China) in blocking solution. In sequential, sections were washed three times with PBS and incubated for 2 h at 37℃ with secondary antibodies (Donkey anti-mouse, 1:500, Beyotime Biotechnology, China) in 0.3% Triton X-100 in PBS in the dark. Lastly, sections were washed three times in PBS and mounted with an antifluorescence quenching mounting medium containing DAPI (Beyotime Biotechnology, China). Pictures were taken under a fluorescence microscope and Image-Pro plus 6.0 software was used to analyze the number of c-Fos positive cells in the PVN.

2.10 Recording of neuronal discharges in the PVN

After the animals recovered for 24 h from MIRI operation, they underwent a craniotomy according to the rat brain atlas under anesthesia. Microwire electrodes were implanted unilaterally at the PVN (antero-posterior: -1.5mm；medio-lateral: ±0.35mm；dorso-ventral: -7.6mm) .A manual micro-thruster was used to slowly push the electrode tip to the PVN or RVLM at a pace of 10 μm/s. Signals were recorded for 5 min after a stable neuron discharge was observed. All data were stored digitally. Neurons were stored with Offline Sorter3 software and the final neuron classification was exported in SPK and FP .pl2 file formats. Then, Neuro Explorer software was used to further analyze the data of the .pl2 files of SPK and local field potential (LFP). Choosing 0-40 Hz, the time was the FP of 300 times the window to calculate the power of its corresponding frequency band. Then, the changes between the groups were observed by comparing the difference between the frequency of neuron firings and LFP in each group.

2.11 Stereotaxic surgery and virus injection

Rats were anesthetized by 3% isoflurane with 99.5% O2, maintained under anesthesia by 1.5-2% isoflurane, and fixed on stereotaxic apparatus (RWD Biotechnology, Shenzhen, China). After incision of the scalp, the skull was exposed and holes were drilled over the targeted areas at the following coordinates from bregma. Virus was bilaterally injected at a rate of 50 nL/min (300 nL per side in PVN, 200 nL per side in RVLM) according to the following coordinates: PVN (antero-posterior: -1.5mm ; medio-lateral: ±0.35mm ; dorso-ventral: -7.6mm), RVLM (antero-posterior: -12.20mm；medio-lateral: ±2.3mm；dorso-ventral: -9.6mm). Removing the needle after 10 min from injection completion. Finally, we sutured the scalp and injected penicillin (200,000U/mL,0.5mL/d) into the rats for three consecutive days to prevent infection.

2.12 Statistical analysis

In this study, all data analysis was performed using Prism 7.0 (GraphPad Software) and SPSS 17.0 software. Data were shown as mean ± SEM. One-way ANOVA with the Turkey test was used for comparison between groups. A value of P <0.05 was considered statistically significant.

3. Results

3.1 EA preconditioning protected myocardial tissue and improved cardiac function in MIRI rats

The changes in the ST segment of the ECG were used to judge whether the MIRI rat model was successfully replicated. We observed that the ST segment of the ECG had significant changes before and after ligation, which decreasing by more than 50% (Fig. 1A). Before the MIRI model was performed, the ST segment displacement values of each group were basically the same while the ST segment of each group was higher than that of the sham group after modeling. Compared with the sham group, the ST segment of the model group increased significantly after 30 min of ligation and 120 min of reperfusion. However, the ST segment of EA group was lower than that of model group (Fig. 1B). Besides, the arrhythmia score of rats showed that the score of the model group was significantly higher than that of the sham group, while the score of the EA group was obviously lower than that of the model group (Fig. 1C).

Next, we observed the morphological changes of myocardial tissue in MIRI rats by HE staining and found that the myocardial fibers in the model group were disorderly arranged, with a large number of inflammatory cells infiltrating. Compared with the model group, the arrangement of myocardial cells was more regular and the degree of bleeding and inflammatory cell infiltration was reduced in the EA group (Fig. 1D).

In addition, CK-MB is a typical marker of myocardial ischemia, and LDH is mainly present in myocardial cells as an important indicator for measuring MIRI. Furthermore, cTnI has been used as a basic indicator for early diagnosis of MI in clinical practice[23,24]. So, we detected the content of these markers in serum. The CK-MB, LDH and cTnI in the model group were higher than those of sham group. The EA intervention reduced the content of those indicators in serum (Fig. 1E, 1F, 1G). The above results showed us that EA at HT7 could significantly reduce myocardial tissue damage and improve arrhythmia in MIRI rats so as to play a protective role for cardiac function.

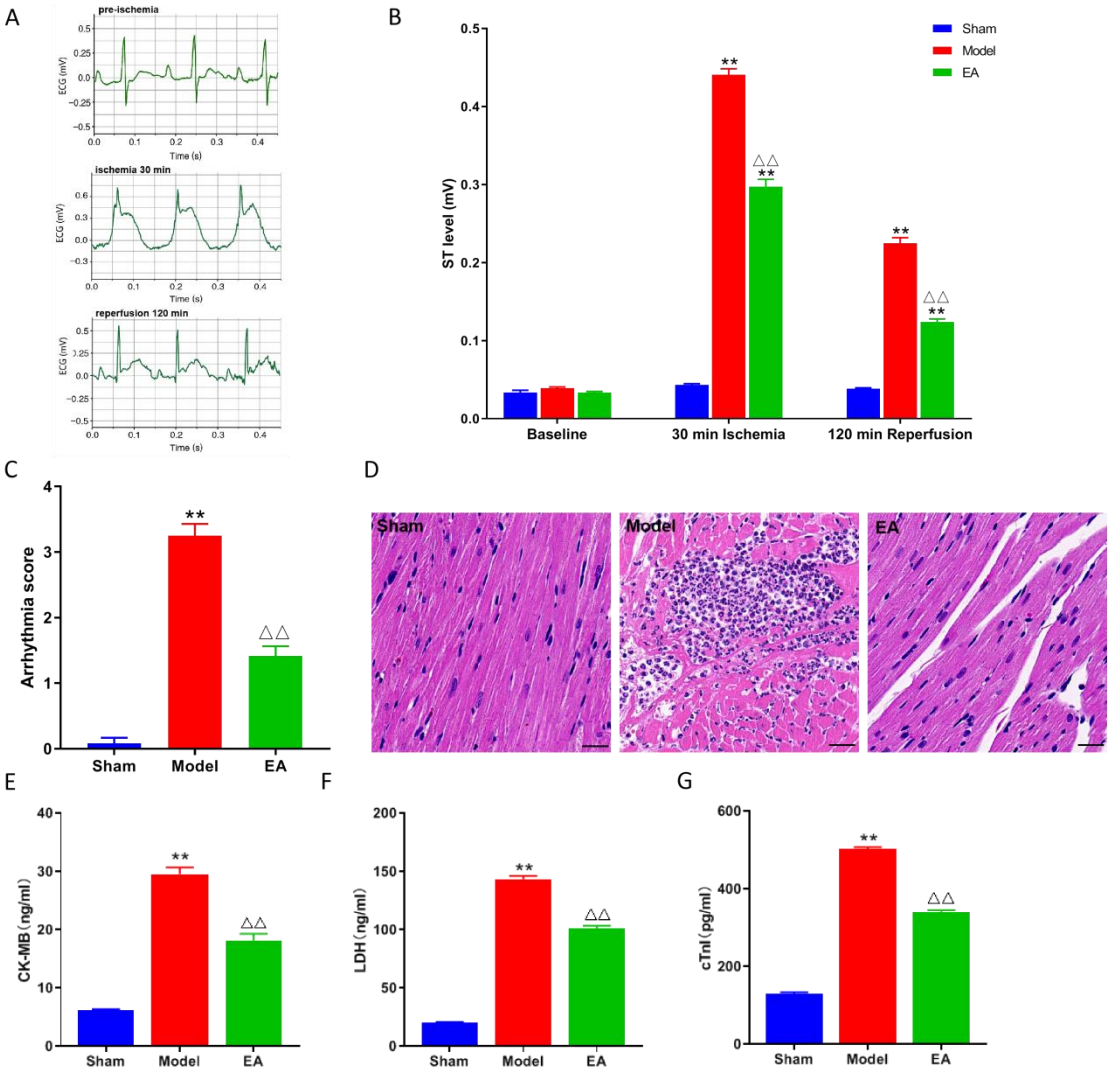

Figure 1. EA preconditioning protected myocardial tissue and improved cardiac function in MIRI rats. (A) the ECG recording of MIRI rats. (B) the statistical analysis of ST deviations of different groups (n=12). (C) the statistical analysis of arrhythmia scores in each group (n=12). (D) hematoxylin-eosin staining results in each group (n=6, scale bar=20um). (E-G) comparison of CK-MB, LDH and cTnI in each group (n=12). All values were displayed as mean ± SEM, one-way ANOVA with Tukey's multiple comparisons test, ***P*<0.01 vs. sham group;△△*P*<0.01 vs. Model group.

3.2 EA pretreatment alleviated MIRI by inhibiting the activity of PVN neurons

To further clarify the mechanism of the PVN in EA improving MIRI, we used immunofluorescence staining and in vivo multi-channel electrophysiological technologies. The proto-oncogene c-Fos is an immediate early gene widely presented in the central nervous system and its encoded c-Fos protein is instantaneously expressed in neurons after synaptic stimulation so as to characterize neuronal activity[25]. Here, we observed the number of c-Fos positive neurons expressed in PVN. Firstly, we determined the positions of PVN according to the brain atlas of rats (Fig. 3A). C-Fos immunoflurescence staining showed that the number of c-Fos+ neurons in PVN in the model group was significantly higher than that in the sham group.

Apparently, the number of c-Fos+ neurons in PVN of the EA group decreased compared to the model group (Fig. 2B, 2C,). Correlation analysis showed a positive correlation between arrhythmia score and the number of c-fos positive neurons (Fig. 2D).

Electrophysiological technology collects the extracellular high-frequency action signals of neurons and the local field potential (LFP) signals of the brain area where the recording electrode is located in real-time to reflect the different activity modes of brain neural network. Therefore, we recorded the neuronal discharges and LFP in the PVN of three groups (Fig. 2E). The total firing frequency of PVN neurons in the model group was significantly increased compared to the sham group. The EA intervention decreased the total frequency compared with the model group (Fig.2F, 2G). In addition, the LFP reflects the cluster activity of neurons; from blue to red indicates that the energy is from small to large. As shown in Fig. 2H, the LFP of PVN in the model group increased compared with the sham group, while the LFP in the EA group decreased compared to the model group. Similarly, correlation analysis showed a positive correlation between arrhythmia scores and the total firing frequency (Fig. 2I). These results were consistent with the findings of c-Fos immunofluorescence staining and suggested that PVN was involved in the process of EA preconditioning to alleviate MIRI. This provided a strong foundation for us to explore the central nervous mechanism of EA pretreatment on MIRI rats.

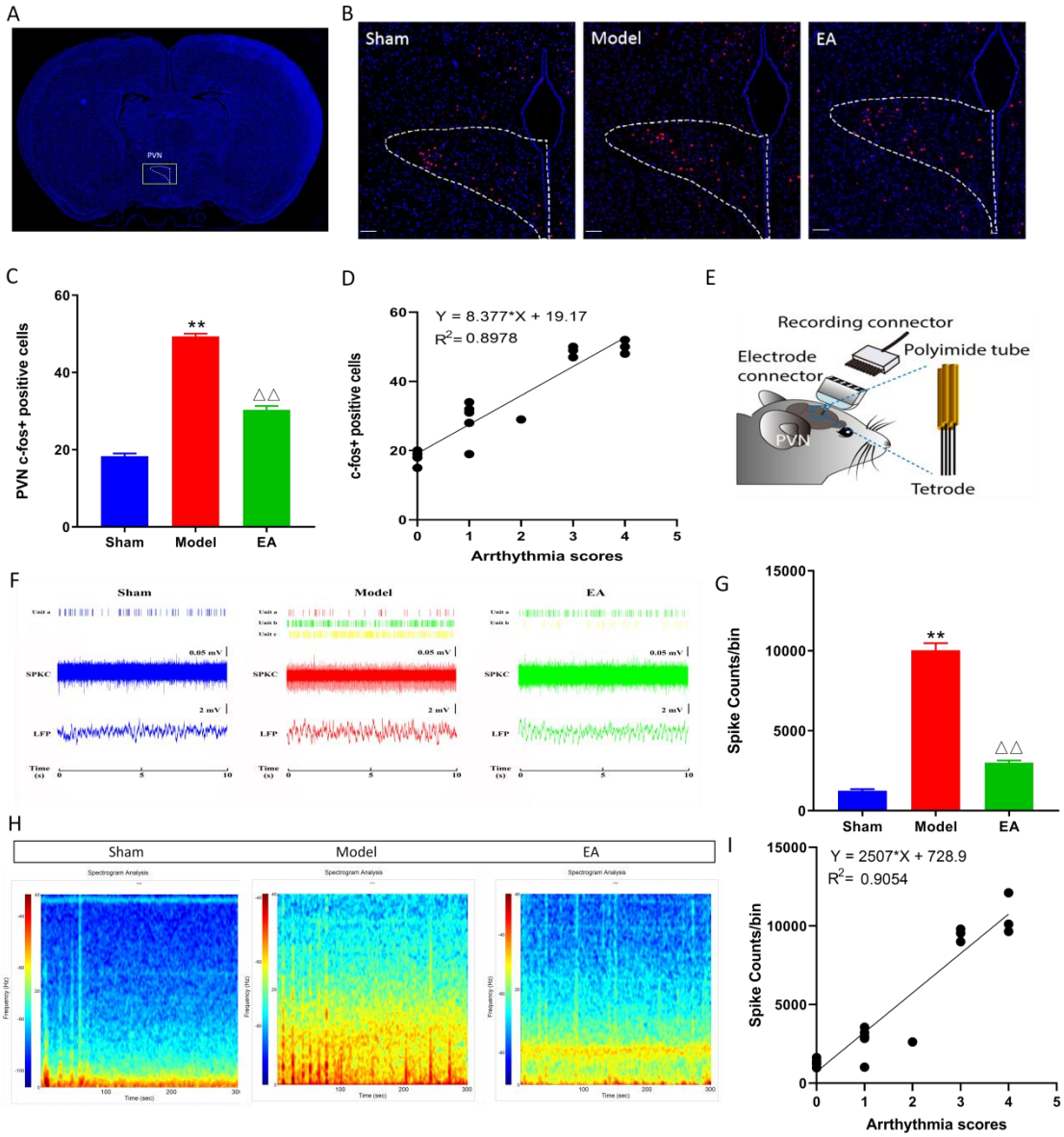

Figure 2. EA pretreatment alleviated MIRI by inhibiting the activity of PVN neurons. (A) the locations of PVN in brain slices according to the brain atlas of rats. (B) the results of c-Fos immunoflurescence staining in PVN of each group (n=6, scale bar=100um). (C) statistical analysis of c-Fos^{+} neurons in PVN (n=6). (D) Correlation analysis between arrhythmia scores and the number of c-fos positive neurons. (E) schematic diagram of electrophysiologiacal operation. (F) action potential and local field potential signals in each group. (G) comparison of total discharge frequency of PVN in each group (n=6). (H) energy maps of local field potentials in PVN of rats in each group (n=6. (I) Correlation analysis between arrhythmia scores and the total firing frequency. All values were shown as mean ± SEM, one-way ANOVA with Tukey's multiple comparisons test, ***P*<0.01 vs. sham group;△△*P*<0.01 vs. Model group.

3.4 Virus tracing revealed the PVN-RVLM neural pathway

Evidence from previous studies have shown that RVLM is an integrated center which receives cardiovascular-related regulatory information from the PVN and nucleus tractus solitarii (NTS), as well as input information from peripheral cardiovascular activity[26,27]. Here,

anterograde and retrograde virus tracers were applied to identify the neural pathway between the PVN and the RVLM. CTB-555 as the retrograde virus was unilaterally injected into RVLM and AAV-hSyn-mCherry as the anterograde virus was unilaterally injected into PVN respectively (Fig. 3A). We found virus labeled neuronal cell bodies in PVN after 7 days from injection of CTB (Fig. 3B). 21 days after the injection in PVN, we discovered the projecting fibers which were labeled with mCherry in RVLM (Fig. 3C). Our experimental results showed that there was a neuronal pathway from PVN to RVLM, which also confirmed by other studies. Therefore, it was possible for us to explain the mechanism of EA alleviating MIRI from the perspective of neural network. Next, we will determine how the PVN-RVLM neural pathway affects MIRI and the specific mechanism involved in EA intervention to improve MIRI. Chemical genetic strategies were used to regulate the PVN-RVLM neural pathway (Fig. 3D) and interventions in each group were implemented after 21 days of virus expression (Fig. 3E).

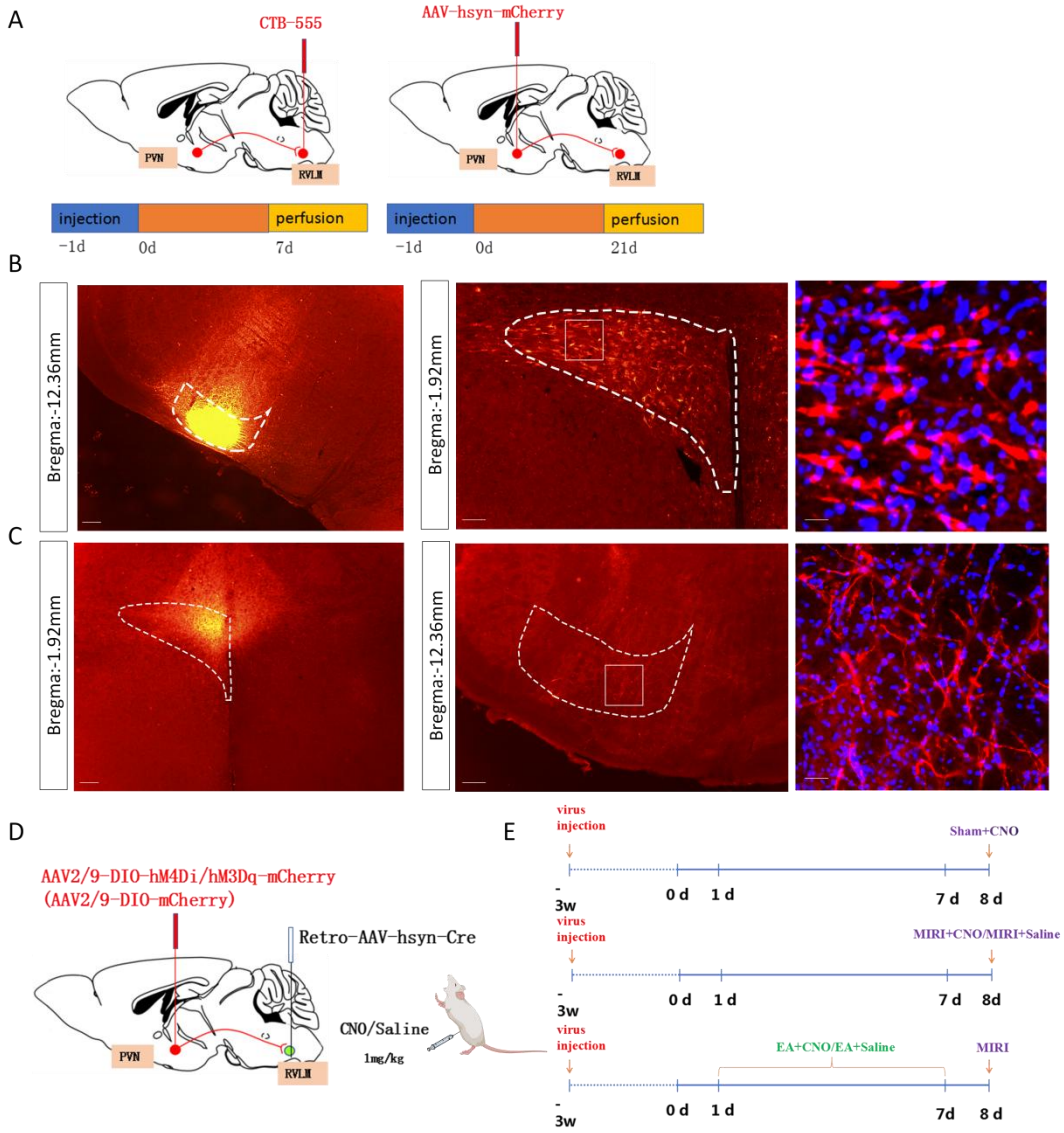

Figure 3. Virus tracing revealed the PVN-RVLM neural pathway. (A) schematic diagram of virus injection (n=3). (B) the site of CTB-555 injection and the projection to PVN. (C) the location of AAV-hsyn-mCherry injection and the projection to RVLM (scale bar=200um, 100um, 50um from left to right). (D) diagram of chemical genetic virus injection. (E) schematics of experimental

design.

3.5 Inhibiting the PVN-RVLM neural pathway alleviated MIRI

We are trying to clarify the effect of inhibiting the PVN-RVLM neural pathway on MIRI rats (Fig. 4A). As shown in Fig. 4B, the location of virus injection was accurate and virus was successfully expressed in the PVN. The ST segments of ECG increased after MIRI model at 30 min of ischemia and 120 min after reperfusion. Compared with the model+mCherry+CNO group, the ST segment decreased significantly in the model+hM4Di+CNO group. To rule out the effect of CNO on MIRI rats, we set up the model+hM4Di+Saline group as a control group. We also observed that the ST segment in model+hM4Di+CNO group was lower than that in model+hM4Di+Saline group (Fig. 4C). Furthermore, inhibiting the PVN-RVLM neural pathway significantly reduced the arrhythmia scores of MIRI rats (Fig. 4D). These results revealed that inhibition of the PVN-RVLM pathway provided a protective effect on cardiac function for MIRI rats.

Next, HE staining showed the morphological changes of myocardial tissue in each group (Fig. 4E). We observed that inhibiting the PVN-RVLM pathway reduced myocardial fiber breakage, myocardial bleeding and inflammatory cell infiltration. In addition, we detected the levels of CK-MB, LDH and cTnI in the serum of each group and found that inhibiting the pathway significantly reduced the levels of the above three indicators in the serum (Fig. 4F, 4G, 4H). We speculate that inhibiting the PVN-RVLM neural pathway has a protective effect which is similar to EA pretreatment on MIRI rats.

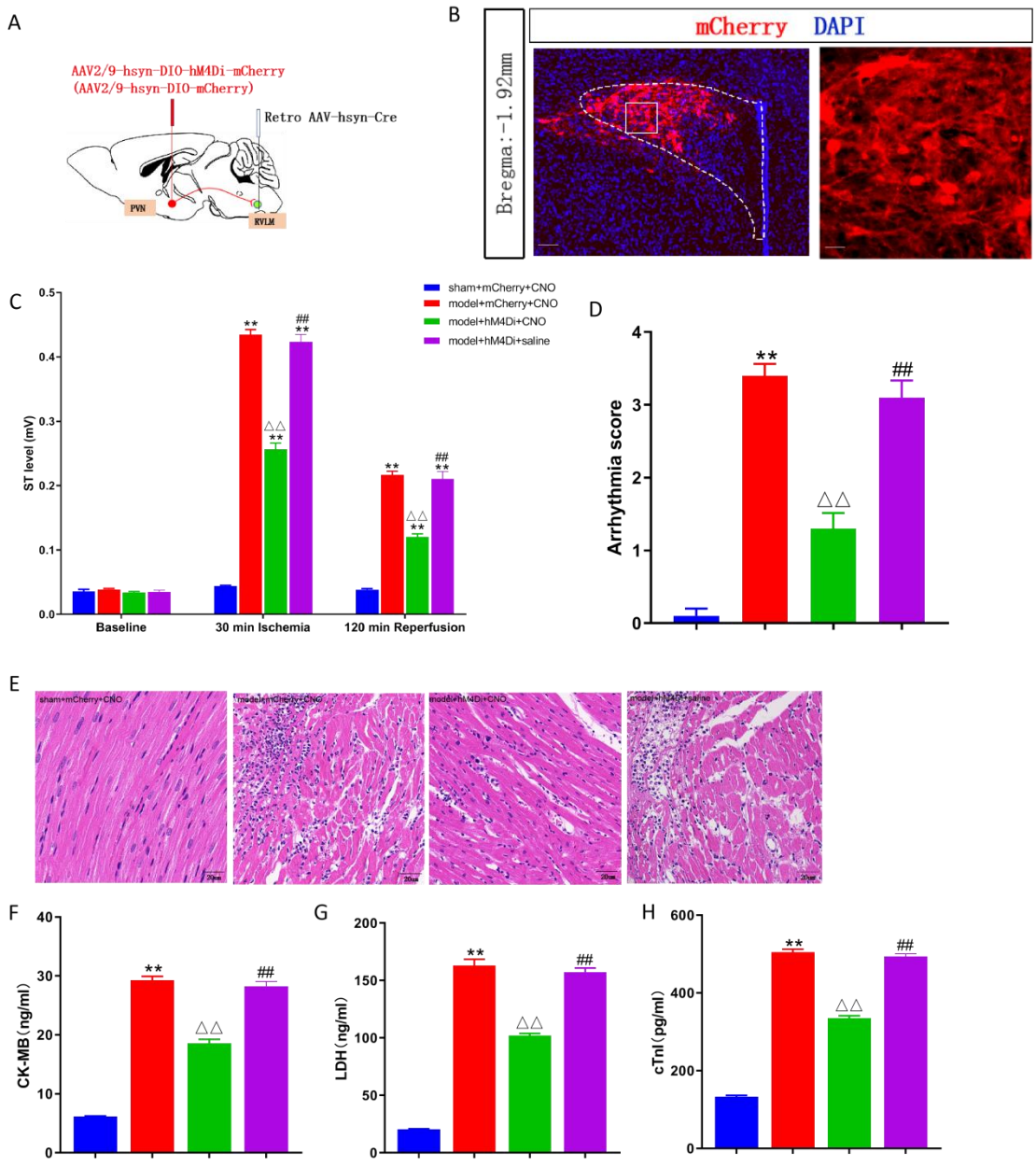

Figure 4. Inhibiting the PVN-RVLM neural pathway alleviated MIRI. (A) the injection of chemical genetic inhibition virus and control virus. (B) the location of virus injection (scale bar=100um, 50um from left to right). (C) the statistical analysis of ST deviations of each group (n=10). (D) comparison of arrhythmia scores among different groups (n=10). (E) the results of hematoxylin-eosin staining in each group (scale bar=20um). (F-H) comparison of CK-MB (n=12), LDH (n=10) and cTnI (n=10) in each group. All values were shown as mean ± SEM, one-way ANOVA with Tukey's multiple comparisons test, ***P*<0.01 vs. sham+mCherry+CNO group;△△*P*<0.01 vs. model+mCherry+CNO group; ## *P*<0.01 vs. model+hM4Di+CNO group.

3.6 Activating the PVN-RVLM neural pathway attenuated the protective effect of EA preconditioning on MIRI

To further explicit the relationship between the PVN-RVLM pathway and EA intervention, we

conducted a chemical genetic strategy to active the pathway (Fig. 5A). Similarly, we confirmed the location of virus injection (Fig. 5B). The segment displacement of ECG in EA+mCherry+CNO group was lower than that in model+mCherry+CNO group at 30 min of ischemia and 120 min after reperfusion. However, activating the PVN-RVLM pathway increased the ST segment displacement compared to the EA+mCherry+CNO group and the EA+hM3Dq+Saline group (Fig. 5C). Besides, activating the pathway increased the arrhythmia scores compared with the EA+mCherry+CNO group and the EA+hM3Dq+Saline group (Fig. 5D). The findings suggested that activating the PVN-RVLM neural pathway antagonized the protective effect of EA preconditioning on MIRI rats.

We simultaneously observed the results of HE staining in each group (Fig. 5E). The staining results of the EA+hM3Dq+CNO group and the model+mCherry+CNO group were similar whic were showing irregular arrangement of myocardial fibers and extensive infiltration of inflammatory cells. Additionally, the comparison of levels of CK-MB, LDH and cTnI in serum of each group showed that activating the pathway increased the levels of these indicators in serum, as to down-regulate the protective effect of EA intervention on MIRI rats (Fig. 5F, 5G, 5H).

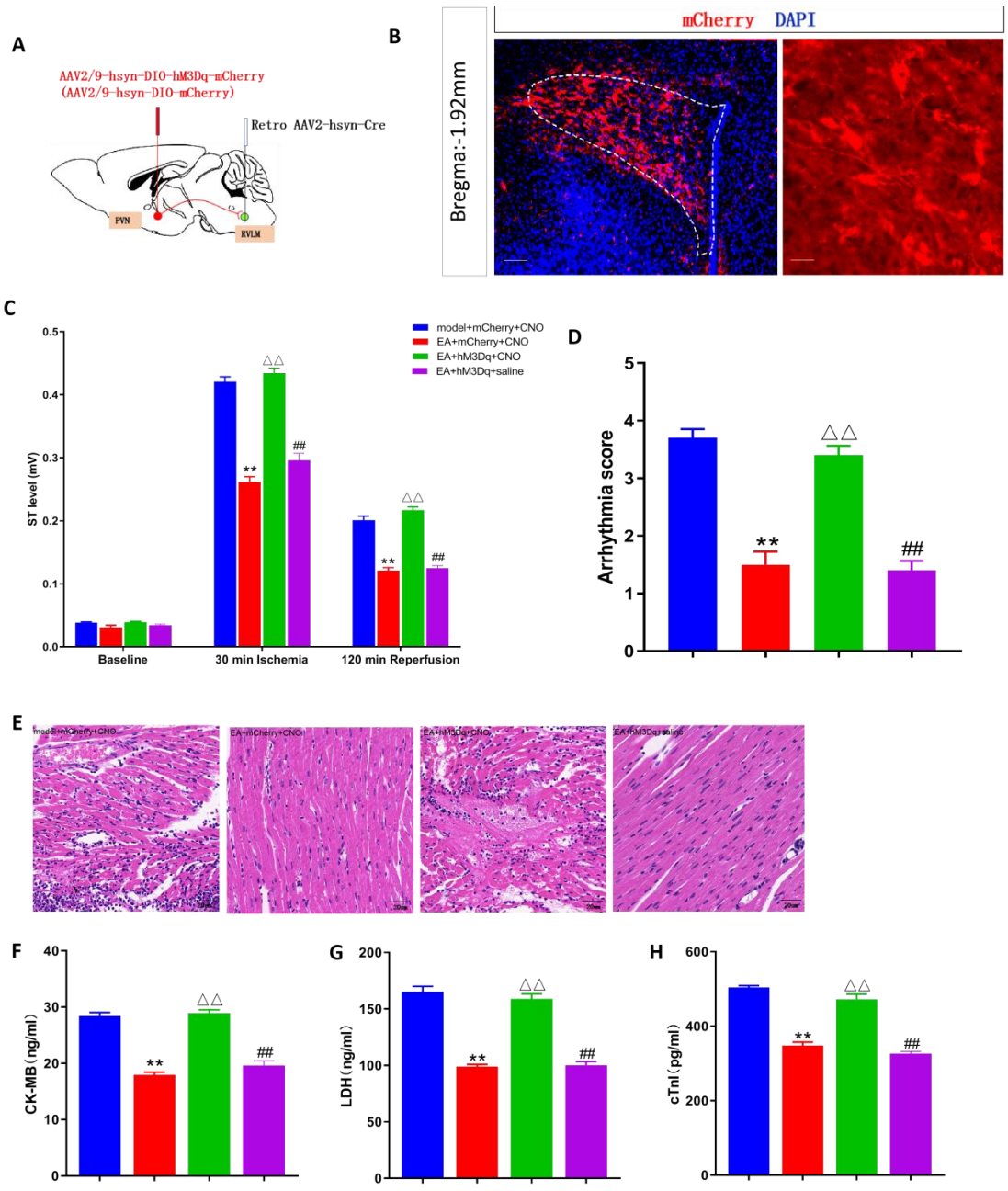

Figure 5. Activating the PVN-RVLM neural pathway attenuated the protective effect of EA on MIRI. (A) the injection of chemical genetic inhibition virus and control virus. (B) the site of virus injection (scale bar=100um, 50um). (C) the statistical analysis of ST deviations of each group (n=10). (D) comparison of arrhythmia scores among different groups (n=10). (E) the results of hematoxylin-eosin staining in each group (scale bar=20um). (F-H) comparison of CK-MB (n=12), LDH (n=10) and cTnI (n=10) in each group. All values were shown as mean ± SEM, one-way ANOVA with Tukey's multiple comparisons test, ***P*<0.01 vs. model+mCherry+CNO group; △△*P*<0.01 vs. EA+mCherry+CNO group; ##*P*<0.01 vs. EA+hM3Dq+CNO group.

4. Discussion

Acupuncture, arguably the most well-konwn complementary and alternative medical

approach, has been practiced in China for over two thousand years and is an effective approach for the relief of the symptoms of angina and palpitations[28]. Electroacupuncture, as a new therapy combining with physical stimulation of nerve stimulation and acupuncture treatment of Chinese medicine, has been widely used in clinical practice and has a positive protective effect against myocardial injury in patients[29-31]. To determine the cardioprotective effect of EA, we established an MIRI model using a LAD coronary artery ligation procedure. The results show that EA preconditioning could inhibit the activity of PVN neurons to alleviate myocardial injury and reduce arrhythmia scores in MIRI rats. Furthermore, the PVN-RVLM neural pathway is an important target for mediating the protective effect of EA pretreatment.

The central nervous system has an extensive physiologic influence on the cardiovascular system, whose heart rate and conduction velocity controlled by the autonomic nervous system. Studies have revealed that reperfusion can cause a higher incidence of ventricular fibrillation than coronary artery occlusion and lethal arrhythmias is one of the main causes of sudden cardiac death[32-34]. In the study, we observed that MIRI induced arrhythmias in rats while EA intervention reduced arrhythmia scores, which partly alleviated myocardial injury. Evidences in clinical practice have also seen the anti-arrhythmia effect of EA treatments[35,36]. However, there are still many doubts about the mechanism of EA pretreatment for arryhthmia after MIRI and autonomic nervous system dysfunction is being a focus. Overactivation of the sympathetic output is considered as an importment mechanism of the arrhythmias, and ameliorating the sympathetic nerve tone after MIRI could potentially reduce the incidence of ventricular arrhythmias[37,38]. PVN, located in the neural nuclei on both sides of the thirs ventricle in the anterior hypothalamic region, is an intergrated site of the neuroendocrine system and the autonomic nervous system, playing a crucial role in regulating electrolyte and fluid balance and cardiovascular activity. We found a strong correlation between the neuronal activity of PVN and arrhythmia score in MIRI rats through in vivo electrophysiological and immunofluorescence methods, indicating that PVN was involved in the pathological process of MIRI, which was consistent with our previous findings[39,40]. Actually, targeted inhibition of sympathetic activity in the PVN can ameliorate peripheral sympathetic activity and reduce the incidence of ventricular arrhythmias[41,42]. EA preconditioning significantly inhibited the activity and reduced the total discharge frequency of PVN, which may be an influential intervention to relieve sympathetic nervous tone to alleviate MIRI.

The cardiac sympathetic afferent reflex belongs to the positive feedback regulatory mechanism which regulates sympathetic and cardiovascular activity[43]. The sympathetic afferent nerve fibers on the surface of the ventricle directly reach PVN and/or reach PVN through the nucleus tractus solitarius. Then, the descending fibers emitted by PVN can reach the intermediate lateral column (IML) of the spinal cord through RVLM or directly reach IML, regulating the activity of sympathetic preganglionic neurons. Such a positive feedback regulation is an advantageous target for EA pretreatment intervention. Interestingly, there are positive markers in PVN and RVLM through virus tracing from acupoint and heart (unpublished), which supports our further research on the implications of PVN and RVLM in EA preconditioning to improve MIRI.

Furthermore, the regulation of cardiovascular activity requires the joint regulation of multiple nuclei and brain regions, and the interconnection, coordination, and cooperation between various levels of cardiovascular regulatory centers play an important role in maintaining

the stability of cardiovascular activity. Studies have shown that the parvicellular divisions of the PVN project to autonomic nuclei in the brainstem and spinal cord and are responsible for activation of the sympathetic nervous system and the regulation of cardiovascular activity[44]. We elucidated the neural projection pathway of PVN-RVLM though virus tracing technology, which was in agreement with the studies of Shafton *et al* (1998) and Xu B *et al* (2012). RVLM is a brain nucleus that critically controls sympathetic outflow and cardiovascular function[45,46]. Given the close functional and structural connection between PVN and RVLM, studies have revealed that photogenetic activation of the PVN-RVLM neural pathway can elicite renal sympathoexcitation, which also contributes to our understanding of central circuitry mechanisms underlying the autonomic imblance associated with cardiovascular diseases[47]. In the study, we found that inhibiting the PVN-RVLM neural pathway through chemical genetics can alleviate MIRI, which was consistent with the protective effect of EA preconditioning. However, activation of the pathway by chemical genetics antagonized the effect of EA intervention. Taken together, the PVN-RVLM neural pathway is involved in MIRI and a considerable way to mediate EA pretreatment to alleviate MIRI.

Unavoidably, some limitations are presented in this work. First, the changes in sympathetic nervous tone in EA pretreatment to alleviate MIRI was not observed. Secondly, there are abundant types of neurons in PVN and RVLM, we didn't determine which specific category of neurons or neuropeptides in PVN and RVLM were involved in the protective effect of EA intervention, fluorescence in situ hybridization and single cell sequencing techniques should be utilized to clarify cell types at the genetic level, thereby revealing particular targets for the mechanism of EA preconditioning to regulate cardiac function. At present, these existing problems are being carefully designed and can be solved in the future.

In conclusion, we demonstrated that EA pretreatment can improve MIRI by inhibiting the PVN neurons projecting to the RVLM. This study provides in-depth insights into the neural mechanism of MIRI and also contributes to further guidance for acupuncture in the treatment of cardiovascular-related diseases.

Authors's contributions

Qi Shu: Experimental operation, Data curation, Methodology, Software, Writing-original. **Jie Zhou:** Experimental operation, Data curation, Methodology, Software. **Bin Zhang:** Experimental operation, Data curation. **Fan Zhang:** Experimental operation. **Xiang Zhou:** Experimental operation. **Yan Wu:** Experimental operation. **Huimin Chang:** Experimental operation. **Ling Hu:** Conceptualization, Writing-review and editing. **Ronglin Cai:** Conceptualization, Methodology, Supervision, Writing-review and editing. **Qing Yu:** Conceptualization, Methodology, Supervision, Writing-review and editing, Project administration.

Conflicts of interest

The authors declare that there is no conflict of interest regarding the publication of this paper.

Data availability

The data that support the findings of this study are available from the corresponding author upon reasonable request.

Ackonwledgments

This work was supported by the National Natural Science Foundation of China (grant number 82074536, 82104999); Natural Science Foundation of Anhui Province (grant number

2108085Y30, 2108085QH364); Anhui Province University Outstanding Top Talent Cultivation Funding Project (grant number gxgwfx2019025)；Anhui Province Excellent Youth Backbone Talent Domestic Visit and Training Program (grant number gxgnfx2022014) and Anhui Province University Scientific Research Project (grant number 2022AH020043, 2022AH030062).

References

[1] Mensah GA, Roth GA, Fuster V., The global burden of cardiovascular diseases and risk factors: 2020 and beyond, J Am Coll Cardiol. 74 (20) (2019) 2529–32.

[2]Feng X-F, et al., Sudden cardiac death in mainland china: a systematic analysis, Circ Arrhythm Electrophysiol. 11 (11) (2018), e006684.

[3]Kalogeris T, et al., Ischemia/reperfusion, Compr Physiol. 7 (1) (2016) 113–170.

[4]Allen, D. G., Orchard, C. H., Myocardial contractile function during ischemia and hypoxia, Circulation Research. 60 (2) (1987) 153-168.

[5]Bugger H, Pfeil K., Mitochondrial ROS in myocardial ischemia reperfusion and remodeling, Biochim Biophys Acta Mol Basis Dis. 1866 (7) (2020) 165768.

[6]Weipan Xu, et al., TRAF1 exacerbates myocardial ischemia reperfusion injury via ASK1-JNK/p38 signaling, J Am Heart Assoc. 8 (21) (2019), e012575.

[7] Yang R, et al., Grpel2 alleviates myocardial ischemia/reperfusion injury by inhibiting MCU-mediated mitochondrial calcium overload, Biochem Biophys Res Commun. 609 (null) (2022) 169-175.

[8]Jennings RB, Historical perspective on the pathology of myocardial ischemia/reperfusion injury, Circ Res. 113 (4) (2013) 428-438.

[9]Yuan J, et al., Correlation between ischemic myocardial injury and inflammatory reaction, and anti-inflammatory effect of acupuncture, Zhen Ci Yan Jiu. 44 (4) (2019) 302-306.

[10] Chen Z H, et al., Research status and prospects on adenosine receptor mechanism of acupuncture for myocardial ischemia, Zhong Guo Zhen Jiu. 40 (11) (2020) 1265-1270.

[11]Cong Chen, et al., Cardioprotective effect of acupuncture for percutaneous coronary intervention-related myocardial injury in patients with coronary artery disease, Medicine. 99 (20) (2020) e20135.

[12] Weixing P, Neurobiological mechanism of acupuncture and moxibustion, Chinese Journal of Traditional Chinese Medicine. 33 (10) (2018) 4281-4297.

[13]Shan Y, et al., An FMRI study of neuronal specificity in acupuncture: the multiacupoint siguan and its sham point, Evid Based Complement Alternat Med. 2014 (null) (2014) 103491.

[14]Peihong Ma, et al., Anarrative review of neuroimaging studies in acupuncture for migraine, Pain Research and Management. 2021 (null) (2021) 9460695.

[15]Qing Y, et al., Effect of electroacupuncture preconditioning on the contents of dopamine and 5-hydroxytryptamine in lateral hypothalamus area and cerebellar fastigial nucleus of rats with myocardial ischemia-reperfusion injury, Zhongguo Zhen Jiu. 41 (1) (2021) 525-530.

[16]Xiaotong Wei, et al., Electroacupuncture preconditionng alleviates myocardial ischemia-reperfusion injury through the hypothalamic paraventricular nucleus-interposed nucleus nerve pathway, Journal of Traditional Chinese Medicine. 42 (3) (2022) 379-388.

[17]Wenjing Cheng, et al., Paraventricular nucleus P2X7 receptors aggravate acute myocardial infarction injury via ROS-induced vasopressin-V1b activation in rats, Neurosci Bull. 37 (5) (2021) 641-656.

[18]Chen, Q. H., et al., Sympathoexcitation by PVN-injected bicuculline requires activation of excitatory amino acid receptors, Hypertension. 42 (4) (2003) 725–731.

[19]Tjen-A-Looi, S C, et al., Paraventricular nucleus modulates excitatory cardiovascular reflexes during electroacupuncture, Scientific Reports. 6 (null) (2016) 25910.

[20] Nishihara, M, et al., Renal denervation enhances GABA-ergic input into the PVN leading to blood

pressure lowering in chronic kidney disease, Auton Neurosci. 204 (null) (2017) 88-97.
[21]Mueller, P. J., et al., Proposed role of the paraventricular nucleus in cardiovascular deconditioning, Acta Physiol Scand. 177 (1) (2003) 27–35.
[22] Zheng, H, et al., A critical role for the paraventricular nucleus of the hypothalamus in the regulation of the volume reflex in normal and various cardiovascular disease states, Curr Hypertens Rep. 24 (7) (2022) 235-246.
[23]You Z, Changsheng M., Clinical significance of serum cTnI, CK-MB, and echocardiography detection in the diagnosis of elderly patients with acute myocardial infarction, Chinese Journal of Gerontology. 39 (03) (2019) 531-533.
[24]Lam L, et al., Effect of macrotroponin on the utility of cardiac troponin I as a prognostic biomarker for long term total and cardiovascular disease mortality, Pathology. 53 (7) (2021) 860-866.
[25]Bullitt E, Expression of c-fos like protein as a marker for neuronal activity following noxious stimulation in the rat, J Comp Neurol. 296(4) (1990) 517- 530.
[26]Charkoudian N, Wallin BG., Sympathetic neural activity to the cardiovascular system: integrator of systemic physiology and interindividual characteristics, Compr Physiol. 4 (2) (2014) 825-850.
[27]Wei Wenwen, et al., Neural pathway between the nucleus accumbens and the rostral ventrolateral medulla in a rat model of anorexia nervosa, J South Med Univ. 40 (5) (2020) 609-615.
[28]Zhao L, et al., Acupuncture as adjunctive therapy for chronic stable angina: a randomized clinical trial, JAMA Intern Med. 179(10) (2019) 1388–1397.
[29]Liu Y, et al., Acupuncture therapy for the treatment of stable angina pectoris: an updated meta-analysis of randomized controlled trials, Complement Ther Clin Pract. 34 (null) (2019) 247–253.
[30]De Lima Pimentel R, et al., Acupuncture for the treatment of cardiovascular diseases: a systematic review, J Acupunct Meridian Stud. 12 (2) (2019) 43-51.
[31]Li RQ, et al., Stable angina pectoris of coronary heart disease treated with different acupuncture and moxibustion therapies: a network Meta-analysis, Zhongguo Zhen jiu. 42 (12) (2022) 1431-8.
[32]Wit AL, Janse MJ., Reperfusion arrhythmias and sudden cardiac death: a century of progress toward an understanding of the mechanisms, Circ Res. 89 (9) (2001) 741–3.
[33] McHugh, N A, et al., Ischemia- and reperfusion-induced ventricular arrhythmias in dogs: effects of estrogen, Am J Physiol. 268 (6 Pt 2) (1995) 2569-73.
[34] Riha, H, et al., Suppression of ischemic and reperfusion ventricular arrhythmias by inhalational anesthetic-induced preconditioning in the rat heart, Physiol Res. 60 (4) (2011) 709-14.
[35]Yangda Li, et al., Comparative effectiveness of acupuncture and antiarrhythmic drugs for the prevention of cardiac arrhythmias: a systematic review and Meta-analysis of randomized controlled trials, Front Physiol. 8 (null) (2017): 358.
[36]Xiangdong Meng, et al., Amiodarone and acupuncture for cardiac arrhythmia: Study protocol for a systematic review, Medicine (Baltimore). 98 (7) (2019), e14544.
[37]Schwartz PJ, Cardiac sympathetic denervation to prevent life-threatening arrhythmias, Nat Rev Cardiol. 11 (6) (2014) 346-53.
[38]Ronglin C., Effect of electroacupuncture on the electrical activity of neurons in the hypothalamic paraventricular nucleus in rats with myocardial ischemia, Acupuncture Research. 43 (07) (2018) 406-413.
[39]Zijian W., Effects of acupuncture at “Neiguan””Shenmen” acupoints on paraventricular nucleus and the

content of serum 5-HT in hyerlipidemia rats after myocardial infarction, Acupuncture Research. 38 (06) (2013) 482-487.

[40]Wang Y, et al., Risk of ventricular arrhythmias after myocardial infarction with diabetes associated with sympathetic neural remodeling in rabbits, Cardiology. 121 (1) (2012) 1–9.
[41]Yugen Shi, et al., Targeted regulation of sympathetic activity in paraventricular nucleus reduces inducible ventricular arrhythmias in rats after myocardial infarction, Journal of Cardiology. 73 (1) (2019) 81-88.
[42]Kang Wang, et al., Effect of TLR4/MyD88/NF-kB axis in paraventricular nucleus on ventricular arrhythmias induced by sympathetic hyperexcitation in post-myocardial infarction rats, J Cell Mol Med. 26 (10) (2022) 1-13.
[43]Malliani A, Montano N., Emerging excitatory role of cardiovascular sympathetic afferents in pathophysiological conditions, Hypertension. 39 (1) (2002) 63-68.
[44]Rossi NF, et al., Neuronal nitric oxide synthase within paraventricular nucleus: blood pressure and baroreflex in two-kidney, one-clip hypertensive rats, Exp Physiol. 95 (8) (2010) 845–857.

[45]Dampney, R. A. L, Functional organization of central pathways regulating the cardiovascular system, Physiol. Rev. 74 (2) (1994).323-64.

[46]Guyenet PG, The sympathetic control of blood pressure, Nat Rev Neurosci. 7 (5) (2006) 335-346.
[47]Satoshi Koba, et al., Sympathoexcitation by hypothalamic paraventricular nucleus neurons projecting to the rostral ventrolateral medulla, J Physiol. 596 (19) (2018) 4581-4595.